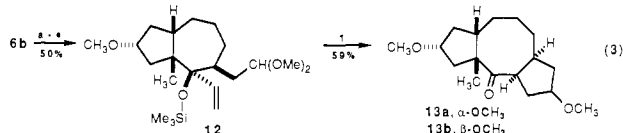


method reported here allows three of the four rings of this alkaloid target to be assembled with *complete* stereocontrol in only five steps from cyclopentanone and, moreover, directly introduces oxidation in the tricyclic product at the two desired sites. The structure of the crystalline dione **10** (mp 56 °C, from hexane) was confirmed by a single-crystal X-ray diffraction study.<sup>18</sup>

Since the products of acetal cyclization–pinacol rearrangements contain a ketone, the sequence reported here can be carried out in an iterative fashion to elaborate two new five-membered rings and accomplish a net two-carbon ring expansion of the starting ketone. The construction of the dicyclopentacyclooctane ring system, a tricyclic skeleton found in a number of biologically important sester- and diterpenes such as the fusicoccins and ophiobolins,<sup>19</sup> illustrates this sequence. Hydroazulenone **6b**, readily available from cyclohexanone (see eq 2), was first elaborated by the efficient stereocontrolled sequence summarized in eq 3 to



\* KMnDS, 0°C, THF, CH<sub>2</sub>=CHCH<sub>3</sub>L, -78° to -50°C. <sup>b</sup> OsO<sub>4</sub>, NaIO<sub>4</sub>, dioxane-H<sub>2</sub>O (3:1), 25°C. <sup>c</sup> MeOH, TsOH (cat.), 25°C. <sup>d</sup> CH<sub>2</sub>=CHLi (15 equiv), THF, -78° to 25°C. <sup>e</sup> Me<sub>3</sub>SiCH<sub>2</sub>CO<sub>2</sub>Et (20 equiv), Bu<sub>4</sub>NF (cat.), 25°C. <sup>f</sup> SnCl<sub>4</sub> (1.1 equiv), CH<sub>2</sub>Cl<sub>2</sub>, -78° to -25°C.

provide **12** as a single diastereomer.<sup>20</sup> Rearrangement of **12** occurred smoothly in the presence of SnCl<sub>4</sub> to give the *cis*-, *anti*-, *cis*-dicyclopentacyclooctanones **13a** and **13b** in a 1:2 ratio and 59% yield after separation on silica gel. The most stable conformation of **13b**, as determined by <sup>1</sup>H NMR NOE experiments and molecular mechanics calculations (MM2), is depicted in structure **14**.

In summary, a wide variety of carbocyclic ring systems can be assembled efficiently and with excellent stereocontrol by the sequential acetal cyclization–pinacol rearrangement strategy reported here. This new chemistry significantly broadens the range of precursors potentially available for assembling carbocyclic skeletons since cyclopentane annulation is coupled with expansion of a preexisting ring. The studies described here, together with our earlier reports<sup>1</sup> and recent disclosures by Trost<sup>22</sup> and Sworin,<sup>23</sup> clearly establish the utility of reaction designs that employ pinacol rearrangements to terminate cationic cyclizations.

**Acknowledgment.** This research was supported by a NIH Jarvis Neuroscience Investigator Award (NS-12389). NMR, mass

(16) Castillo, M.; Loyola, L. A.; Morales, G.; Singh, I.; Calvo, C.; Holland, M. L.; MacLean, D. B. *Can. J. Chem.* **1976**, *54*, 2893. Loyola, L. A.; Morales, G.; Castillo, M. *Phytochem.* **1979**, *18*, 1721.

(17) These alkaloids have not been prepared by total synthesis. Two approaches were recently disclosed. See: St. Laurent, D. R.; Paquette, L. A. *J. Org. Chem.* **1986**, *51*, 3861. Mehta, G.; Rao, K. S. *J. Chem. Soc., Chem. Commun.* **1987**, 1578.

(18) *R<sub>F</sub>* = 5.9%, *R<sub>wF</sub>* = 6.5%. Details are provided as Supplementary Material.

(19) For a review, see: Cordell, J. *Phytochemistry* **1974**, *13*, 2343. Leading references to recent synthesis efforts in this area can be found in: Rigby, J. H.; Senanayake, C. *J. Org. Chem.* **1987**, *52*, 5635.

(20) The stereochemical outcome of these transformations is consistent with existing precedent;<sup>21</sup> the stereochemistry of the acetal side chain was rigorously established by 2D <sup>1</sup>H NOE experiments.

(21) Heathcock, C. H.; Tice, C. M.; Germroth, T. C. *J. Am. Chem. Soc.* **1982**, *104*, 6081.

(22) Trost, B. M.; Lee, D. C. *J. Am. Chem. Soc.* **1988**, *110*, 6556.

(23) Sworin, M.; Neumann, W. L. *J. Org. Chem.* **1988**, *53*, 4894.

spectral, and X-ray instrumentation employed in this study were purchased with the assistance of NSF Shared Instrumentation Grants. We especially wish to acknowledge Dr. Joseph Ziller for carrying out the X-ray analysis of **10**, Dr. Shoumo Chang for assistance with 2D NMR experiments, and Dr. Matthew Abelman for numerous insightful suggestions.

**Supplementary Material Available:** A typical procedure for the rearrangement step and experimental data for the X-ray diffraction study of **10** (7 pages). Ordering information is given on any current masthead page.

### Three-Dimensional Heteronuclear NMR of <sup>15</sup>N-Labeled Proteins

Dominique Marion,<sup>†</sup> Lewis E. Kay,<sup>†</sup> Steven W. Sparks,<sup>‡</sup> Dennis A. Torchia,<sup>‡</sup> and Ad Bax<sup>\*†</sup>

Laboratory of Chemical Physics, NIDDK  
Bone Research Branch, NIDR  
National Institutes of Health  
Bethesda, Maryland 20892

Received September 12, 1988

The introduction of two-dimensional (2D) NMR<sup>1</sup> has made it possible to determine solution structures of small proteins.<sup>2</sup> Although the 2D approach greatly reduces spectral overlap, many ambiguities remain in the analysis of 2D protein NMR spectra because of coincident or nearly coincident chemical shifts. Commonly used procedures to solve this type of problem rely on the fact that the chemical shifts of many protons show different pH and temperature dependence. Another, more elegant approach utilizes 3D NMR<sup>3-6</sup> to remove the problem of degenerate chemical shifts. Homonuclear 3D techniques, combining *J* connectivity and NOE information, have recently been demonstrated for small proteins, clearly demonstrating the power of this approach.<sup>6,7</sup> However, for proteins larger than about 15 kD, the *J* connectivity transfer step in such a 3D experiment rapidly loses its efficiency, severely decreasing sensitivity. Here the use of a very sensitive 3D experiment is demonstrated for unraveling the regular protein NOESY spectrum. This method requires <sup>15</sup>N labeling of the protein, a relatively simple procedure for bacterially overexpressed proteins. High-quality 3D NMR spectra can be obtained in a few days, without excessive demands for data processing or data storage.

The NOESY–HMQC pulse scheme we utilized (Figure 1) is slightly different from the scheme proposed very recently by Fesik and Zuiderweg,<sup>8</sup> permitting observation of NOE's to C $\alpha$ H protons that resonate very close to the H<sub>2</sub>O resonance. The *t*<sub>1</sub> and *t*<sub>3</sub> dimensions represent the time variables in a regular NOESY experiment; during the *t*<sub>2</sub> dimension the NH protons are labeled with their <sup>15</sup>N chemical shifts. Therefore, a projection of the 3D spectrum onto the *F*<sub>1</sub>–*F*<sub>3</sub> plane corresponds to the regular amide region of a 2D NOESY spectrum. However, individual *F*<sub>1</sub>–*F*<sub>3</sub>

<sup>†</sup> Laboratory of Chemical Physics, NIDDK.

<sup>‡</sup> Bone Research Branch, NIDR.

(1) Ernst, R. R.; Bodenhausen, G.; Wokaun, A. *Principles of Nuclear Magnetic Resonance in One and Two Dimensions*; Clarendon: Oxford, 1987.

(2) Wuethrich, K. *NMR of Proteins and Nucleic Acids*; Wiley: New York, 1986.

(3) Griesinger, C.; Sørensen, O. W.; Ernst, R. R. *J. Magn. Reson.* **1987**, *73*, 574.

(4) Griesinger, C.; Sørensen, O. W.; Ernst, R. R. *J. Am. Chem. Soc.* **1987**, *109*, 7227.

(5) Vuister, G. W.; Boelens, R. *J. Magn. Reson.* **1987**, *73*, 328.

(6) Oschkinat, H.; Griesinger, C.; Kraulis, P. J.; Sørensen, O. W.; Ernst, R. R.; Gronenborn, A. M.; Clore, G. M. *Nature (London)* **1988**, *332*, 374.

(7) Vuister, G. W.; Boelens, R.; Kaptein, R. *J. Magn. Reson.* **1980**, *80*, 176.

(8) Fesik, S. W.; Zuiderweg, E. R. P. *J. Magn. Reson.* **1988**, *78*, 588.

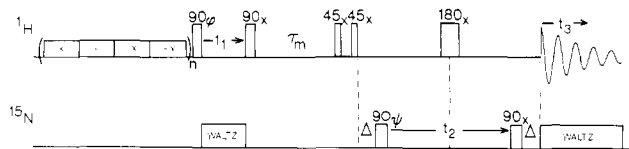


**Figure 1.** Pulse scheme of the 3D NOESY-HMQC experiment. The  $^1\text{H}$  carrier is positioned in the center of the amide region, and the observe transmitter is used in the low power mode for generating a DANTE type presaturation of  $\text{H}_2\text{O}$ .<sup>14</sup> The phase cycling used is as follows:  $\phi = x, y, -x, -y$ ;  $\psi = 4(x), 4(-x)$ ;  $\text{Acq}_1 = 2(x), 4(-x), 2(x)$ , with data for odd- and even-numbered scans stored separately. The entire sequence is repeated with  $\psi$  incremented by  $90^\circ$  to obtain complex data in the  $F_2$  dimension.

planes show NOE connectivities only for amide protons with a particular  $^{15}\text{N}$  chemical shift. Suppression of the intense  $\text{H}_2\text{O}$  resonance is accomplished in two stages; first the water resonance is slightly attenuated by the use of a very weak presaturating field (equivalent to  $\gamma B_2 \approx 12$  Hz on the water resonance) and second

an off-resonance  $45^\circ\text{-}\tau\text{-}45^\circ$  pulse is used at the end of the NOESY mixing period to minimize the excitation of the remaining  $\text{H}_2\text{O}$  magnetization.

Figure 2 presents two (out of 64) NOESY slices taken from the most crowded region of the 3D spectrum at  $^{15}\text{N}$  shifts of 121.4 and 122.3 ppm. A slice taken at 121.8 ppm and the comparable region of a regular NOESY spectrum are shown in the supplementary data. The 3D spectrum has been recorded in 2.5 days on a NT-500 spectrometer, for a 1.8 mM solution of  $^{15}\text{N}$  labeled Staphylococcal nuclease (S. Nase) complexed with pdTp and  $\text{Ca}^{2+}$ , in 90% $\text{H}_2\text{O}/10\%\text{D}_2\text{O}$ , pH 6.5, 37  $^\circ\text{C}$ . The sensitivity of the 3D spectrum is similar to that of the conventional NOESY spectrum, but the severe overlap present in the 2D spectrum is almost completely removed. The 3D spectrum is particularly useful for tracing out the backbone (NH/NH and NH/C $\alpha$ H) connectivities in the protein and such correlations have been labeled in Figure 2. On the basis of this 3D spectrum and on a number of other isotopic labeling and double labeling techniques<sup>9-11</sup> we have been

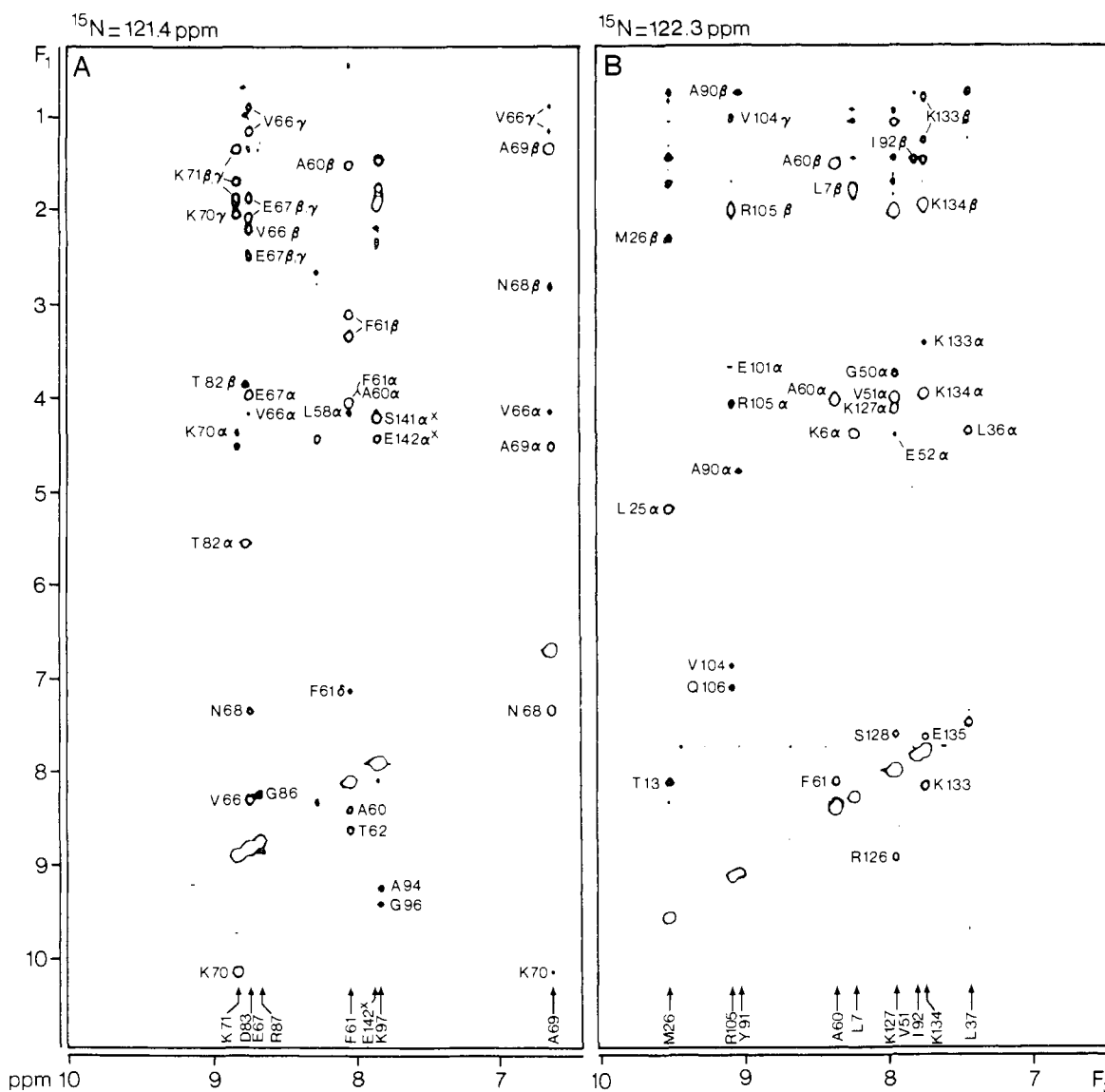


**Figure 2.** Two adjacent  $F_1/F_3$  slices taken from the 500-MHz 3D spectrum of S. Nase, recorded with the scheme of Figure 1, for an NOE mixing time of 125 ms. The spectrum was recorded without using dummy scans; instead a single  $90^\circ$  pulse was used prior to the first scan of each ( $t_1, t_2$ ) value to accomplish a "steady state". The  $^1\text{H}$  and  $^{15}\text{N}$  carrier frequencies were positioned at 8.67 and 120.0 ppm downfield from the resonances of trimethylsilyl propionate and liquid ammonia, respectively. (A) Slice taken for an  $^{15}\text{N}$  chemical shift ( $F_2$ ) of 121.4 ppm and (B) for  $F_2 = 122.3$  ppm. The spectrum results from a  $32 \times 128 \times 256$  complex data matrix, with acquisition times of 23, 21, and 64 ms in the  $t_1, t_2$ , and  $t_3$  dimension, respectively. 16 scans (twice the minimal number) were acquired per  $t_1/t_2$  value and the total measuring time was 2.6 days. Zero filling was used in all three dimensions to yield a  $64 \times 256 \times 512$  matrix for the absorptive part of the 3D spectrum. Digital resolution in the final spectrum is 22, 24, and 8 Hz per point in the  $F_1, F_2$ , and  $F_3$  dimension, respectively. Digital filtering used was the following:  $60^\circ$  shifted sine bell ( $t_3$ ) and double shifted ( $60^\circ$  at the beginning and  $10^\circ$  at the end) in the  $t_1$  and  $t_2$  dimensions. A linear base line correction routine was used in the  $F_3$  dimension only. Data have been processed with commercially available software (New Methods Research Inc., Syracuse, NY) supplemented by simple home-written routines for digital filtering and Fourier transformation<sup>13</sup> in the  $t_2$  dimension.

able to obtain virtually complete backbone assignments for the 156-residue protein, which will be reported elsewhere.

Major practical problems with 3D spectroscopy are the long measuring time needed to get sufficient digitization in the  $F_1$  and  $F_2$  dimensions of the 3D spectrum and the large size of the 3D matrix. We have used folding of some of the resonances in both the  $F_1$  and  $F_2$  dimensions and employed an unfolding procedure<sup>12</sup> in the  $F_1$  dimension (based on shifting the  $F_1$  carrier position during data processing<sup>13</sup>) to obtain maximum resolution with a relatively small number of  $t_1$  and  $t_2$  increments. The minimum measuring time also depends on the number of scans needed for phase cycling or each set of  $t_1, t_2$  values and on the overhead time needed to write the data to disk at the end of an acquisition. In principle, replacing the first  $^1\text{H}$  90° pulse by a frequency-selective pulse could reduce the minimum measuring time (or increase digitization),<sup>3</sup> but this would eliminate informative correlations from the 3D spectrum. We therefore believe that the heteronuclear 3D experiment discussed here is best executed in a nonselective fashion. The sensitivity of the heteronuclear 3D technique is excellent, and resonance overlap in the S. Nase 3D spectrum is minimal, despite the relatively coarse digitization. The three-dimensional NMR experiment reported here should be applicable to proteins significantly larger than S. Nase.

**Acknowledgment.** This work was supported by the Intramural AIDS Antiviral Program of the Office of the Director of the National Institutes of Health. L.E.K. and D.M. acknowledge financial support from the Medical Research Council, Canada, and from the CNRS/NIH exchange agreement, respectively. We thank Rolf Tschudin for technical support.

**Supplementary Material Available:** Three figures giving the projection of the 3D spectrum on the  $F_2/F_3$  plane, a  $F_1/F_3$  slice taken at  $F_2 = 121.8$  ppm, and an identical region of the regular 2D NOESY spectrum (4 pages). Ordering information is given on any current masthead page.

(9) Kainoshi, M.; Tsuji, T. *Biochemistry* **1982**, *21*, 6273.

(10) Griffey, R. H.; Redfield, A. G. *Q. Rev. Biophys.* **1987**, *19*, 51.

(11) Torchia, D. A.; Sparks, S. W.; Bax, A. *Biochemistry* **1988**, *27*, 5135.

(12) Reference 1, pp 337-338. Bax, A.; Griffey, R. H.; Hawkins, B. L. *J. Magn. Reson.* **1983**, *55*, 301.

(13) Kay, L. E.; Marion, D.; Bax, A. *J. Magn. Reson.*, submitted.

(14) Morris, A. G.; Freeman, R. *J. Magn. Reson.* **1978**, *29*, 433.

### A General Solution To Implementing the $4\pi$ Participation of 1-Aza-1,3-butadienes in Diels-Alder Reactions: Inverse Electron Demand Diels-Alder Reactions of $\alpha,\beta$ -Unsaturated *N*-Benzenesulfonyl Imines

Dale L. Boger\*<sup>1</sup> and Annette M. Kasper

Department of Chemistry, Purdue University  
West Lafayette, Indiana 47907

Received November 16, 1988

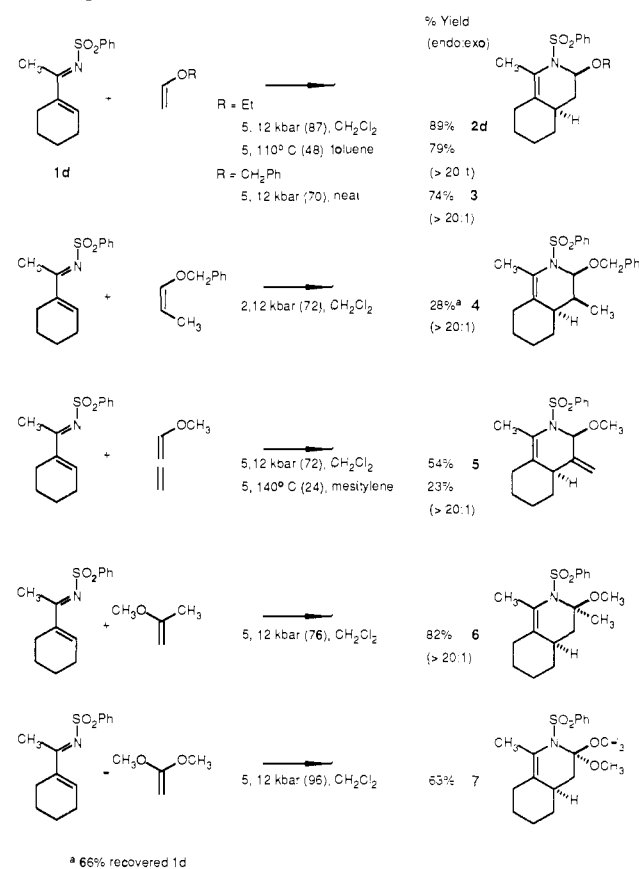
The Diels-Alder  $4\pi$  participation of simple  $\alpha,\beta$ -unsaturated imines is rarely observed and typically suffers low conversions, competitive imine addition, and/or imine tautomerization precluding  $[4+2]$  cycloaddition.<sup>2</sup> Consequently only a limited number of 1-aza-1,3-butadiene structural variations and modified or restricted reaction conditions have been introduced that have permitted the productive  $4\pi$  participation of selected  $\alpha,\beta$ -unsaturated imines in  $[4+2]$  cycloaddition reactions.<sup>3-7</sup> In the conduct

(1) National Institutes of Health research career development award recipient (CA 01136), 1983-1988. Alfred P. Sloan research fellow, 1985-1989.

(2) Boger, D. L.; Weinreb, S. M. *Hetero Diels-Alder Methodology in Organic Synthesis*, Academic Press: Orlando, FL, 1987.

(3) Hwang, Y. C.; Fowler, F. W. *J. Org. Chem.* **1985**, *50*, 2719.

### Scheme I



of synthetic efforts on natural and synthetic quinoline-5,8-quinones including streptonigrone,<sup>8</sup> we have examined alternative approaches to predictably control and accelerate the intermolecular  $4\pi$  participation of 1-aza-1,3-butadienes in  $[4+2]$  cycloaddition reactions. The complementary N-1 or C-3 substitution of an  $\alpha,\beta$ -unsaturated imine with an electron-withdrawing substituent would be expected to accentuate the electron-deficient nature of the 1-aza-1,3-butadiene and accelerate its potential  $[4+2]$  cycloaddition reaction with electron-rich dienophiles in LUMO<sub>diene</sub>-controlled Diels-Alder reactions.<sup>2</sup> In addition, a bulky, electron-withdrawing N-1 1-aza-1,3-butadiene substituent would be expected to preferentially decelerate 1,2-imine addition relative to  $[4+2]$  cycloaddition and convey  $[4+2]$  cycloaddition product stability to the reaction conditions while enhancing the electron-deficient nature of the diene. Herein we detail a comparative study of the  $4\pi$  participation of  $\text{N}^1$ -substituted  $\alpha,\beta$ -unsaturated imines in LUMO<sub>diene</sub>-controlled Diels-Alder reactions which has revealed the general, well-defined  $4\pi$  participation of  $\alpha,\beta$ -unsaturated *N*-benzenesulfonyl imines in regio- and endo-specific inverse electron demand Diels-Alder reactions suitable for the diastereoselective preparation of substituted *N*-benzenesulfonyl-1,2,3,4-tetrahydropyridines.

Representative results of initial studies employing stable imine derivatives of 1-acetylcyclohexene<sup>9</sup> are summarized in eq 1 and

(4) Ito, Y.; Miyata, S.; Nakatsuka, M.; Saegusa, T. *J. Am. Chem. Soc.* **1981**, *103*, 5250.

(5) Poncin, B. S.; Frisque, A.-M. H.; Ghosez, L. *Tetrahedron Lett.* **1982**, *23*, 3261.

(6) Ihara, M.; Kirihara, T.; Kawaguchi, A.; Fukumoto, K.; Kametani, T. *Tetrahedron Lett.* **1984**, *25*, 4541.

(7) (a) Whitesell, M. A.; Kyba, E. P. *Tetrahedron Lett.* **1984**, *25*, 2119. (b) Nenitzescu, C. D.; Cioranescu, E.; Birladeanu, L. *Commun. Acad. Rep. Populare Romine* **1958**, *8*, 775. (c) Baydar, A. E.; Boyd, G. V.; Lindley, P. F.; Watson, F. *J. Chem. Soc., Chem. Commun.* **1979**, 178. (d) Alberola, A.; Gonzalez, A. M.; Gonzalez, B.; Laguna, M. A.; Pulido, F. *J. Tetrahedron Lett.* **1986**, *27*, 2027. (e) Komatsu, M.; Takamatsu, S.; Uesaka, M.; Yamamoto, S.; Ohshiro, Y.; Agawa, T. *J. Org. Chem.* **1984**, *49*, 2691.

(8) Herlt, A. J.; Rickards, R. W.; Wu, J.-P. *J. Antibiot.* **1985**, *38*, 516.